HHS Public Access

Author manuscript

*Nat Biotechnol*. Author manuscript; available in PMC 2009 October 01.

Published in final edited form as:

*Nat Biotechnol*. 2009 April ; 27(4): 387–394. doi:10.1038/nbt.1531.

# Substrate-Free High-Throughput Screening Identifies Selective Inhibitors for Uncharacterized Enzymes

**Daniel A. Bachovchin**[1,2], **Steven J. Brown**[2,3], **Hugh Rosen**[2,3], and **Benjamin F. Cravatt**[1,2,*]

[1]The Skaggs Institute for Chemical Biology, The Scripps Research Institute, La Jolla, CA 92037, USA

[2]Department of Chemical Physiology, The Scripps Research Institute, La Jolla, CA 92037, USA

[3]The Scripps Research Institute Molecular Screening Center, The Scripps Research Institute, La Jolla, CA 92037, USA

## Abstract

Target-based high-throughput screening (HTS) is essential for the discovery of small-molecule modulators of proteins. Typical screening methods for enzymes rely on extensively tailored substrate assays, which are not available for targets of poorly characterized biochemical activity. Here, we report a general, substrate-free platform for HTS that overcomes this problem by monitoring the reaction of broad-spectrum, activity-based probes with enzymes using fluorescence polarization. We show that this platform is applicable to enzymes from multiple mechanistic classes, regardless of their degree of functional annotation, and can be coupled with secondary competitive activity-based proteomic assays to rapidly determine the specificity of screening hits. Using this platform, we identified the bioactive alkaloid emetine as a selective inhibitor of the uncharacterized cancer-associated hydrolase RBBP9. We furthermore show that the detoxification enzyme GSTO1, also implicated in cancer, is inhibited by several electrophilic compounds found in public libraries, some of which display high selectivity for this enzyme.

Advancements in robotics technologies, coupled with the generation and assembly of large libraries of structurally diverse small-molecules, have led to a tremendous expansion of high-throughput screening (HTS) programs in both academia and industry1, 2. A variety of screens have been introduced that range from more classical *in vitro* substrate assays for enzyme inhibitors to *in situ* screens that profile cellular phenotypes. A key advantage of HTS is the potential to mine large compound libraries to discover novel chemotypes that possess interesting and often unanticipated biological activities. Examples of such chemotypes include enzyme inhibitors that act by unprecedented mechanisms3, receptor agonists with high specificity and in vivo efficacy4, and compounds that kill cancer cells by inducing an atypical cell death pathway5. Public small-molecule libraries also contain a large number of bioactive natural products (http://pubchem.ncbi.nlm.nih.gov/), many of



*To whom correspondence should be addressed: cravatt@scripps.edu.

**Author contributions.** D.A.B. performed experiments. D.A.B., S.J.B, H.R. and B.F.C. designed experiments and analyzed data. D.A.B. and B.F.C. wrote the paper.

which act by still ill-defined mechanisms, and HTS offers a potentially attractive strategy to discover protein targets for these compounds.

Essential to the success of any target-based HTS program is the development of a high-quality screen. Key factors that must be satisfied include – an accurate and, ideally, homogeneous biochemical readout of protein activity, robust assay reproducibility between wells and plates, adequate sensitivity to identify compounds with weak activity, and affordability. Meeting these criteria can be challenging, even for well-studied proteins, and is even more daunting for proteins with poorly characterized biochemical activities. As a consequence, the unannotated portion of the human proteome, which by some estimates may amount to 30−50% of all human proteins6, has, to date, remained outside of the general scope of HTS programs.

A large fraction of uncharacterized mammalian proteins are enzymes. Genetic and cell biology studies have begun to link some of these enzymes to important physiological and disease processes7-9. However, our lack of understanding of the substrates utilized by uncharacterized enzymes impedes the development of standard HTS assays for inhibitor screening. Sequence homology, on the other hand, can often assign these enzymes to specific mechanistic classes, and this knowledge has been used to develop chemical proteomic tools for their characterization. Prominent among these chemo-proteomic methods is activity-based protein profiling (ABPP)10, 11.

ABPP makes use of reactive chemical probes to covalently modify the active sites of enzymes. ABPP probes typically exploit conserved catalytic and/or recognition elements in active sites to target a large number of mechanistically related enzymes. Incorporation of fluorescent and/or biotin tags into probe structures enables detection and enrichment/identification, respectively, of protein targets. ABPP has been applied to discover enzyme activities in a wide range of (patho)physiological processes, including cancer12-15, infectious disease16, and nervous system signaling17. Interestingly, a large number of enzymes identified by ABPP in these studies are uncharacterized (i.e., they lack known substrates)13, 15, 17, 18. By performing ABPP experiments in a competitive mode, where small-molecules are screened for their ability to block probe labeling of enzymes19, lead inhibitors have been generated for some uncharacterized enzymes20, 21. An important feature of this approach is that the potency and selectivity of inhibitors can be concurrently optimized because compounds are profiled against a large number of mechanistically related enzymes in parallel.

A major shortcoming of competitive ABPP studies has, however, been their limited throughput. Assays are typically readout using one-dimensional SDS-PAGE gels, which are not suitable for HTS. As a consequence, only modest-sized compound libraries (200−300 compounds) can be screened using current competitive ABPP methods21. Here, we have addressed this major limitation by developing a fluorescence polarization (FluoPol) platform for competitive ABPP. We show that this platform is HTS-compatible and can be readily adapted for use with different classes of enzymes and ABPP probes. Moreover, we further report the use of FluoPol-ABPP to discover selective inhibitors for two cancer-related enzyme targets, the hydrolytic enzyme RBBP9 and the thioltransferase GSTO1.

## Results

### FluoPol-ABPP assay development for RBBP9

As an initial target for screening by FluoPol-ABPP, we selected the putative hydrolytic enzyme retinoblastoma-binding protein-9 (RBBP9). RBBP9 was originally identified in a screen for gene products that confer resistance to the growth-inhibitory effects of TGF-beta17. RBBP9 has also been reported to bind the retinoblastoma (RB) protein, transform rat liver epithelial cell lines, and show elevated expression in primary human liver tumors7. These data suggest that RBBP9 could play an important role in cancer. Nonetheless, to date, the biochemical functions of RBBP9 have remained enigmatic. Structural genomics22 and functional proteomics17 studies indicate that RBBP9 is a member of the serine hydrolase superfamily, but neither substrates nor selective inhibitors for the enzyme have yet been identified22. Our goal was therefore to establish a FluoPol-ABPP HTS assay to screen for inhibitors of human RBBP9.

We took advantage of the interaction between purified recombinant RBBP9 and the serine hydrolase-directed activity-based probe fluorophosphonate (FP)-rhodamine (Supplementary Fig. 1)12, 23. The basis for monitoring this reaction by FluoPol is summarized as follows. Labeling of RBBP9 by FP-rhodamine will greatly increase the apparent mass of the fluorescent probe, resulting in the maintenance of a strong FluoPol signal when compared to unreacted, free probe (Fig. 1). Importantly, this difference in FluoPol should be detectable in a homogeneous assay format. Titrations of RBBP9 and FP-rhodamine confirmed these predictions and led to the identification of conditions (2 μM RBBP9, 75 nM FP-rhodamine) where enzyme labeling generated a strong, time-dependent increase in FluoPol signal (Fig. 2a). No labeling was observed with a mutant RBBP9 enzyme where the serine nucleophile was converted to alanine (S75A) (Fig. 2a).

We reasoned that an RBBP9 inhibitor would slow the rate of enzyme labeling, which would, in turn, reduce the FluoPol signal (Fig. 1a). However, because reversible inhibitors should reduce the extent of enzyme labeling only for a limited period of time, it was essential to perform the inhibition assay under kinetically controlled conditions (i.e., before the enzyme labeling reaction had reached completion19). Following the time-course of the FP-rhodamine-RBBP9 reaction identified a time point (45 min) where partial enzyme labeling yielded a strong FluoPol signal that displayed a robust *Z*' factor of 0.71 (Fig. 2a). Kinetic analysis by gel-based ABPP, where probe-enzyme reactions are quenched at various time points, separated by SDS-PAGE, and quantified by in-gel fluorescence scanning, confirmed partial (∼60% of maximal) labeling of RBBP9 at the 45 min time point (Supplementary Fig. 2). At this kinetically tractable time point, either reversible or irreversible inhibition of RBBP9 labeling should be detectable by a significant drop in fluorescence polarization signals. To further substantiate this premise, we performed FluoPol assays in the presence of a biotinylated FP probe (FP-biotin24) at a concentration matching its $IC_{50}$ value for RBBP9 inhibition as predicted from gel-based competitive ABPP assays (Fig. 2b). An ∼50% reduction in FluoPol signal was observed for RBBP9 in the presence of FP-biotin (Fig. 2c), indicating that the FluoPol-ABPP assay can detect partially inhibited RBBP9.

### HTS for RBBP9 inhibitors by FluoPol-ABPP

We next performed a FluoPol-ABPP screen for RBBP9 inhibitors in a 384-well format using a library of 18,974 small-molecules. On each plate, we included control reactions without added small-molecules or RBBP9 to set high and low boundaries for FluoPol signals, respectively. The assay performance was consistent across plates, with robust *Z*' factors and signal-to-noise (S:N) ratios suitable for HTS (Supplementary Fig. 3). From this screen, we identified 35 primary hits, defined as compounds that reduced the FluoPol signal for FP-rhodamine labeling of RBBP9 by > 50% relative to control reactions (Fig. 3a **and** Supplementary Table 1). These hits included several quinones (e.g., **2**), α,β-unsaturated ketones (UKs) (e.g., **3**), a bis-thiocarbonate (**4**), and the bioactive natural product emetine (**1)** (Fig. 3b).

### Secondary proteomic competitive ABPP assays

A key advantage of FluoPol-ABPP is that the activity-based probe used for HTS can also be incorporated into secondary gel-based screens to rapidly rule out false-positive and non-selective primary hits. We first evaluated 31 of the hit compounds (20 μM) against purified RBBP9 by gel-based ABPP (Fig. 3c, upper panel). Methoxy arachidonyl fluorophosphonate (MAFP) is an irreversible inhibitor of several serine lipases25, but does not block FP-rhodamine labeling of RBBP9 (Fig. 3c), and was therefore included as a negative control. This assay revealed that 20 of the 31 hits blocked FP-rhodamine labeling of RBBP9 by >50%. The remaining 'false-positive' hits likely derive from common HTS artifacts such as fluorescent compound interference or instrumentation error.

The 20 active compounds (20 μM) were then evaluated by competitive ABPP in two complex proteomes - the membrane fraction of mouse brain doped with exogenous human RBBP9 (Fig. 4a) and the soluble fraction of RBBP9-transfected COS-7 cells (Fig. 4b), which showed robust expression of RBBP9 (Supplementary Fig. 4). Here, we selected competitive ABPP assay conditions where the majority of the serine hydrolases were not yet completely labeled so that either reversible or irreversible inhibition of most enzymes could be monitored collectively at a single time point (Supplementary Fig. 5). These convenient screens identified emetine (**1**) as a highly selective inhibitor of RBBP9. Emetine inhibited FP-rhodamine labeling of RBBP9 with an $IC_{50}$ of 7.8 μM (Fig. 3e), but, remarkably, did not block the labeling of any other hydrolase when tested at concentrations up to 1 mM (Fig. 4d).

The proteomic ABPP assays also permitted categorization of the other 19 active compounds into two groups (Fig. 4c). First, thirteen compounds, including **2-4**, were non-selective, inhibiting multiple hydrolases in proteomes (Fig. 4a,b). These compounds possess potentially thiol-reactive chemotypes (such as quinones and UKs) and inhibited similar 'off-target' hydrolases, including the maleimide-sensitive enzyme monoacylglycerol lipase (MAGL)26 (Fig. 4a,b). This finding suggests that these compounds may inhibit RBBP9 by alkylation of an active site cysteine residue (see below). Second, six compounds exhibited membrane-sensitive activity. Exemplifying this category, compound **5** blocked labeling of nearly all hydrolases in the soluble COS-7 proteome (Fig. 4b), but had little detectable activity against membrane-associated hydrolases (Fig. 4a). This result flagged these

compounds as potential aggregation-based inhibitors, which are common false-positives in HTS screens27, 28. The resistance of membrane, but not soluble enzymes to this class of inhibitors could reflect an attenuation of their aggregation properties due to interactions with endogenous lipid bilayers, since detergents are also known to quench compound aggregation28, 29. Consistent with the premise, we found that increasing concentrations of the surfactant Pluronic F-127 significantly impaired the inhibitory activity of compound **5,** but did not diminish the inhibitory activity of emetine (Supplementary Fig. 6).

## SAR of emetine and RBBP9 inhibition

Emetine induces a broad range of cellular effects, including an increase in alternative splicing of the Bcl-x gene30, antagonism of α2-adrenergic receptors31, inhibition of protein synthesis, and cell death. Few protein targets of emetine, however, have been discovered. Emetine's cytotoxic activity has historically been linked to blockade of protein translation32, presumably through direct interactions with the ribosome33; however, less toxic structural analogues of emetine, such as the anti-ameobasis drug dehydroemetine, maintain equivalent inhibitory activity on protein translation32. These findings suggest the existence of still unidentified protein targets that are specifically inhibited by emetine. To explore the structure-activity relationship for inhibition of RBBP9 by emetine, we screened ∼75 commercially available compounds possessing structural features similar to emetine by competitive ABPP (Fig. 3d, Supplementary Figs. 7 and 8, and Supplementary Table 2). Only two additional compounds, the natural product alkaloids cephaeline (**1a**, Fig. 3d) and tubusoline (**1c**, Fig. 3d), inhibited RBBP9, albeit with reduced potency relative to emetine (Fig. 3e and Supplementary Fig. 7). Notably, dehydroemetine (**1b**), which only differs from emetine by the presence of one double bond, failed to inhibit RBBP9 at concentrations up to 200 μM (Fig. 3e and Supplementary Fig. 7). These data thus designate RBBP9 as the first protein target, to our knowledge, that is selectively inhibited by emetine, but not dehydroemetine.

## Mechanistic characterization of RBBP9 inhibitors

From our secondary proteomic ABPP assays, we suspected that several screening hits, such as the electrophilic quinone **2**, might irreversibly inhibit RBBP9. As further evidence of covalent inhibition, we noticed that compounds possessing two electrophilic moieties, such as compound **4,** dimerized recombinant RBBP9 as judged by the detection of a higher migrating species by SDS-PAGE (Fig. 3b, lower panel). Consistent with a covalent mode of inhibition, blockade of FP-rhodamine labeling of RBPP9 by **2** was not reversed by gel filtration of the **2**-RBPP9 reaction (Fig. 5a). In contrast, gel filtration of an emetine-RBBP9 reaction completely restored the FP-rhodamine labeling of RBBP9 (Fig. 5a). These data indicate that emetine is a reversible RBBP9 inhibitor.

Quinones are well-known alkylating agents34, and we reasoned that Cys163, which resides two residues away from the catalytic His165 in the human RBBP9 (hRBBP9) active site22, might serve as a potential site of irreversible alkylation. Interestingly, this residue is an arginine in other RBBP9 orthologues, including those from horse, rat, and mouse. This predicts that other RBBP9 orthologues should be resistant to inhibition by **2**. Indeed, we found that mouse RBBP9 (mRBBP9) displays a ∼50-fold reduced sensitivity to **2** (Fig. 5b),

being inhibited only at concentrations where **2** indiscriminately blocks FP-rhodamine labeling of most serine hydrolases in proteomes (Supplementary Fig. 9). Further supporting Cys163 as the site of alkylation for **2** in hRBBP9, a Cys163Arg (C163R) mutation rendered this enzyme similarly insensitive to **2** (Fig. 5b). Emetine, however, exhibited similar activity against hRBBP9 (wt), hRBBP9 (C163R), and mRBBP9 (Fig. 5c). These results thus provide mechanistic insights to explain how alkylating agents inhibit hRBPP9 and suggest further that emetine likely serves as a general inhibitor of mammalian RBBP9 orthologues.

## GSTO1 inhibitor discovery by FluoPol-ABPP

To test whether FluoPol-ABPP could be applied to a second, mechanistically distinct enzyme class that reacted with a different activity-based probe, we assayed the oxidoreductase glutathione S-transferase omega 1 (GSTO1). GSTs are cellular detoxifying enzymes that metabolize endogenous compounds, chemotherapeutic agents, and by-products of oxidative stress, and have recently gained attention as potential anticancer drug targets35. GSTO1, in particular, is overexpressed in human cancer cell lines that show enhanced aggressiveness15 and chemotherapeutic resistance36. GSTO1 is an atypical GST that utilizes a catalytic cysteine nucleophile37, which renders it sensitive to generic thiol-alkylating agents, such as *N*-ethylmaleimide38. However, selective GSTO1 inhibitors have not yet been identified. We previously discovered that GSTO1 reacts strongly with sulfonate ester (SE) activity-based probes15, which target a broad swath of metabolic enzymes in proteomes.

Under conditions similar to the RBBP9 assay, the reaction of GSTO1 (1 μM) and a SE-rhodamine probe (75 nM) (Supplementary Fig. 1) generated a robust, time-dependent increase in fluorescence polarization signal (Fig. 6a). No labeling was seen with a mutant GSTO1 enzyme where the catalytic cysteine was converted to alanine (C32A), or in the presence of 1 mM glutathione, a known inhibitor of probe labeling15 (Fig. 6a). A time-course of the SE-rhodamine-GSTO1 reaction identified a time point (90 min) where partial GSTO1 labeling yielded a strong polarization signal with a robust *Z*' factor of 0.67. Under these conditions, we screened 2,000 compounds (5 μM) in 384-well format and identified 38 primary hits that reduced the fluorescence polarization signal by >50% (Supplementary Table 3). This 2,000 compound library also contained six primary hits from the RBBP9 screen. Interestingly, five of these six compounds also registered as hits for GSTO1, with the only exception being emetine (**1**), which did not block probe labeling of GSTO1.

Among the GSTO1 primary hits were, not surprisingly, 20 potentially thiol-reactive compounds, including the thiol-reactive RBBP9 inhibitor **3**, the proton pump inhibitor omeprazole (**6**), the disulfide **7**, and the α-chloroacetamide **8** (Fig. 6b). In addition, we identified 11 phenols, a chemotype known to inhibit GSTs39, including the antibiotic rifampicin (**9**) (Fig. 6b). Gel-based ABPP with recombinant GSTO1 confirmed the inhibitory activity for a representative subset of compounds. **7** and **8** potently inhibited GSTO1 with $IC_{50}$ values < 0.4 μM (Fig. 6b). Gel filtration studies indicated that these inhibitors act by an irreversible mechanism, in contrast to **6** and **9**, which behaved as lower potency, reversible inhibitors of GSTO1 (Fig. 6c).

To assess the selectivity of **6**−**9**, we evaluated these compounds by competitive ABPP using the cytosolic proteome of a human breast cancer cell line (MDA-MB-231) that expresses high endogenous levels of GSTO1. (Fig. 6d,e). Here, we again selected assay conditions where the majority of the probe targets were not yet completely labeled (Supplementary Fig. 5). We also included the previously identified RBBP9 inhibitors emetine (**1**), quinone **2,** and UK **3,** in this analysis. Each of the hit compounds inhibited GSTO1 at 20 μM, although **6** and **9** were considerably less potent than **2, 3, 7,** and **8** (Fig. 6d). At this concentration, however, **2, 7,** and **8** also inhibited the SE-rhodamine labeling of several other proteins in the MDA-MB-231 proteome, while compound **3** appeared to activate labeling of an 80 kDa band. We have previously identified this protein as type 2 tissue transglutaminase40, a protein that is activated by several cofactors (GTP, calcium)41. In contrast, emetine (**1**) did not inhibit the labeling of GSTO1 or any of the other SE-rhodamine targets. Interestingly, when we lowered the concentration of inhibitors to 1 μM, compound **8** maintained strong inhibition of GSTO1, while the activities of compounds **2, 3, 6, 7,** and **9** were lost (Fig. 6e). Moreover, at this concentration, **8** showed good selectivity for GSTO1 in the MDA-MB-231 proteome (Fig. 6e). We finally confirmed that **8** was a potent inhibitor of GSTO1 ($IC_{50}$ value of 120 nM) using an *S*-4-(nitrophenacyl)glutathione substrate assay42 (Supplementary Fig. 10). These data indicate that the tempered α-chloroacetamide electrophile of **8** offers a window for potent and selective inhibition of GSTO1. The other GSTO1 hits that showed potent inhibition of purified enzyme, but greatly reduced activity in proteomes (e.g., compound **7**), are likely reactive with many proteins and metabolites in the cellular environment, thereby reducing potency for GSTO1 and ablating any selectivity window for GSTO1.

## Discussion

Complete genome sequences have revealed that eukaryotic and prokaryotic organisms universally possess a huge number of uncharacterized proteins6. Even for proteins that may be considered ‘annotated’, we have yet, in most instances, to achieve a complete understanding of their biochemical, cellular, and physiological functions. A central component of efforts to annotate the proteome is the development of selective pharmacological probes to perturb the function of individual proteins in native biological settings. HTS has assumed a prominent role in small-molecule probe development in both academia and industry6, as exemplified by the National Institutes of Health Molecular Libraries Screening initiative (http://nihroadmap.nih.gov/molecularlibraries/). The success of such endeavors hinges on the advancement of high-quality screens, which is particularly challenging for proteins of poorly characterized biochemical function. Here, we have introduced FluoPol-ABPP as a general solution to this problem for a potentially wide range of enzymes.

We analyzed the cancer-associated hydrolase RBBP9 by FluoPol-ABPP and discovered that this protein is inhibited by the natural product emetine. Notably, emetine did not inhibit any of the other serine hydrolases detected in our proteomic ABPP studies. The RBBP9-emetine interaction furthermore displayed a tight structure-activity relationship, with chemical analogues, such as dehydroemetine, lacking activity. These data suggest that RBBP9 could

be a relevant target to explain the molecular mechanisms underlying the bioactivity of emetine and related ipecac alkaloids, and, conversely, these natural products may offer useful probes for exploring the enzymatic functions of RBBP9 in biological systems. Our further finding that RBBP9, as well as several other serine hydrolases, were susceptible to inactivation by thiol-reactive electrophilic compounds (quinones, disulfides) suggests that this class of enzymes might be regulated by endogenous pathways for post-translational modification of cysteines (e.g., nitroyslation43, oxidation44, electrophilic modification45).

We also applied FluoPol-ABPP to discover the α-chloracetamide **8** as a selective, covalent inhibitor for a second cancer-associated enzyme, GSTO1. Importantly, RBBP9 and GSTO1 are mechanistically distinct enzymes (serine hydrolase and reductase/thioltransferase, respectively) targeted by difference classes of ABPP probes (FP and SE, respectively). The successful application of FluoPol-ABPP to discover both reversible and irreversible inhibitors for each of these proteins underscores the versatility and generality of this platform. Indeed, for RBBP9, it is difficult to conceive of another HTS-compatible biochemical assay, since despite much effort22, substrates have not yet been identified for this enzyme. In the case of GSTO1, a limited number of substrate assays have been developed, but these are not well-suited for HTS [e.g., UV absorbance assays at short wavelengths (305 nm) where many small-molecules exhibit intrinsic absorbance42). Thus, FluoPol-ABPP should prove valuable not only for uncharacterized enzymes, but also for enzymes with substrate assays that are not readily adaptable to an HTS format.

A handful of complementary assays have also been introduced to expand the range of proteins amenable to HTS. For instance, FluoPol platforms have recently been described that use aptamers46 or reversibly binding small-molecules47 as probes. Aptamers have the advantage of being potentially applicable to proteins of poorly characterized function, although, in principle, an individual aptamer would need to be developed for each target (or set of structurally related targets). In contrast, individual ABPP probes can target more than 100 enzymes that are structurally quite divergent13, 17, 48, making them amenable for screening a large fraction of the proteome. ABPP also offers straightforward secondary assays to rapidly assess compound activity and selectivity in complex biological samples, such that non-specific compounds (e.g., compounds **2 and 7**; see Figs. 4 and 6, Supplementary Fig. 11) and compounds showing odd behavior (e.g., compound **5**) can be discarded in favor of inhibitors that selectively block their intended target in proteomes (e.g., emetine and compound **8** for RBBP9 and GSTO1, respectively). These secondary, proteomic selectivity assays are more difficult to perform with reversibly binding small-molecule probes.

There are some limitations of FluoPol-ABPP that merit further discussion. First, this method is only applicable to enzymes for which cognate activity-based probes have been developed. While many important enzyme classes fall into this category (hydrolases, proteases, kinases, oxidoreductases)10, 11, several others remain outside the current scope of ABPP. It is also important to recognize that blockade of probe labeling may not, in all cases, equate with inhibition of an enzyme's catalytic activity. Secondary substrate assays can readily address this concern for some enzymes (e.g., as we showed for GSTO1), but may not be available for poorly characterized enzymes (e.g., RBBP9). Nonetheless, competitive ABPP has been

successfully used to develop potent and selective inhibitors for many enzymes10, 11 and, we anticipate, in most instances, that probe labeling will serve as a valid surrogate for the catalytic activity of enzymes. In addition, FluoPol-ABPP requires a substantial amount of purified protein (∼ 4 nmol/384-well plate), which may prove challenging for certain enzymes (e.g., transmembrane enzymes). The quantity of enzyme could, of course, be substantially reduced by performing the assay in 1536-well format or by conducting labeling reactions for a longer period of time. Regardless, in cases where protein quantity is not limiting, FluoPol-ABPP is quite cheap, since the quantity of probe used per assay is negligible (0.3 nmol/384-well plate). We thus anticipate that continued efforts to advance the large-scale production of proteins, such as those embodied by structural genomics initiatives49, should dovetail nicely with ongoing chemical proteomic studies to provide a growing number of target proteins and probes for the construction of FluoPol-ABPP HTS assays. The pharmacological tools that emerge from these screens should propel future investigations that aim to functionally annotate the proteome.

## METHODS

### Materials

FP-biotin24, FP-rhodamine23, SE-rhodamine40, and *S*-4-(nitrophenacyl)glutathione42 were synthesized following previously described protocols. Emetine, glutathione, methyl arachidonoyl fluorophosphonate (MAFP), omeprazole, and rifampicin were purchased from Sigma. Compounds **2**, **4**, and **5** were purchased from Ryan Scientific, and compounds **3**, **7**, **8**, and **69**−**138** were purchased from BioFocus DPI. Emetine analogues **1a-g** were obtained from the National Cancer Institute. Screening compound libraries are described in the Supplementary Methods online.

### Recombinant Protein Expression and Purification

Full-length cDNA encoding human RBBP9 in pcDNA3 (Invitrogen) was a gift of the Cheresh lab (UCSD), and full-length cDNA encoding mouse RBBP9 was purchased from Open BioSystems. GSTO1 was obtained as an expressed sequence tag from Invitrogen. These genes were subconed into pTrcHisB (Invitrogen). Point mutants were generated using the Quikchange Site-Directed Mutagenesis Kit (Stratagene). The constructs were expressed in BL21(DE3) *E. coli* and purified as described in the Supplementary Methods.

### FluoPol-ABPP Assays

The RBBP9 FluoPol-ABPP assay was performed in a 384-well format. Briefly, 10 μL of recombinant RBBP9 (2.2 μM) in assay buffer (50 mM Tris-HCl [pH 8.0], 150 mM NaCl, 0.01% Pluronic F-127 [Invitrogen]) was added to test compound and negative control wells, and 10 μL assay buffer alone was added to positive control wells. Compounds were then added to test compound wells and DMSO to control wells by pintool, and plates were then incubated at 25 °C for 30 minutes. 1.1 μL of FP-rhodamine (750 nM in assay buffer; 75 nM final concentration in FluoPol assay) was added to all wells. The plates were incubated for additional 45 min at 25 °C and then read on an Envision platereader (Perkin Elmer).

The GSTO1 FluoPol-ABPP assay was similarly performed in a 384-well format. Briefly, 10 μL of GSTO1 (1.1 μM) in assay buffer was added to test compound and negative control wells, and 10 μL of assay buffer alone to positive control wells. Compounds were added to test compound wells and DMSO to control wells by pintool. Plates were then incubated at 25 °C for 30 minutes. 1.1 μL of SE-rhodamine (750 nM in assay buffer) was added to all wells. The plates were incubated for 90 minutes at 25 °C and then read on an Envision platereader.

### Gel-Based ABPP experiments with recombinant enzyme

Initial secondary gel-based ABPP analysis of primary hits was performed under the same conditions as the corresponding FluoPol-ABPP assay. Briefly, recombinant RBBP9 (2 μM) in assay buffer was incubated with DMSO or indicated compound (20 μM) for 30 min at 25 °C before the addition of FP-rhodamine at a final concentration of 75 nM in 50 μL total reaction volume. The reaction was incubated for 45 min at 25 °C, quenched with 2× SDS-PAGE loading buffer, boiled for 5 min at 90 °C, separated by SDS-PAGE, and visualized in-gel using a flatbed fluorescence scanner (Hitachi). The percentage activity remaining was determined by measuring the integrated optical density of the bands. Similarly, recombinant GSTO1 (1 μM) in assay buffer was incubated with DMSO or indicated compound (20 μM) for 30 min at 25 °C in a 50 μL total reaction volume. SE-rhodamine (75 nM final concentration) was then added, and the reaction was incubated at 25 °C for 90 min before it was similarly quenched and analyzed. For the determination of compound $IC_{50}$ values using ABPP, the overall procedure remained the same but with conditions that enabled the use of less enzyme (400 nM RBBP9, 1 μM FP-rhodamine, 10 min; 400 nM GSTO1, 1 μM SE-rhodamine, 20 min). $IC_{50}$ values were determined from dose-response curves from three trials at each inhibitor concentration (0.1−100 μM) using Prism software (GraphPad). For experiments involving gel-filtration of recombinant enzyme to test compound reversibility, discussed in detail in the Supplementary Methods, the reactions were set-up similarly with the exception that a fraction of the enzyme-inhibitor mixture was passaged over a Sephadex G-25M column (GE Healthcare) prior to the reaction with the ABPP probe.

### Competitive ABPP assays in proteomes

The mouse brain membrane proteome, prepared as described in Supplementary Methods, was diluted to 1 mg/mL in phosphate-buffered saline (PBS). Recombinant RBBP9 (400 nM) was added for comparison where indicated. Similarly, the soluble proteome of transfected COS-7 cells, prepared as described in Supplementary Methods, was diluted to 1 mg/mL in phosphate-buffered saline (PBS). These proteomes were pre-incubated with either DMSO or candidate inhibitor at the indicated concentration in a 50 μL reaction volume for 30 min at 25 °C. FP-rhodamine was then added at a final concentration of 1 μM. After 10 min, the reactions were quenched and analyzed as described above. The soluble fraction of the human breast cancer cell line MDA-MB-231, prepared as described in Supplementary Methods, was diluted to 2 mg/mL in PBS. The proteome was pre-incubated with either DMSO or candidate inhibitor at the indicated concentration in a 50 μL reaction volume for 30 min at 25 °C, and SE-rhodamine was added at a final concentration of 5 μM. After 1 hr, the reactions were quenched and analyzed as described above.

### GSTO1 Substrate Assay

This assay was performed as previously described42 as detailed in the Supplementary Methods.

## Supplementary Material

Refer to Web version on PubMed Central for supplementary material.

## Acknowledgments

We thank the Cravatt laboratory for helpful discussions. We are grateful to Stephan Schürer and Pierre Baillargeon for help purchasing emetine analogues, and Sarah Tully for assistance with the synthesis of 4NPG. This work was supported by the N.I.H. (CA132630, MH084512), an N.S.F. Predoctoral Fellowship (D.A.B.), and the Skaggs Institute for Chemical Biology.

## References

1. Inglese J, et al. High-throughput screening assays for the identification of chemical probes. Nat Chem Biol. 2007; 3:466–479. [PubMed: 17637779]
2. Shelat AA, Guy RK. Scaffold composition and biological relevance of screening libraries. Nat Chem Biol. 2007; 3:442–446. [PubMed: 17637770]
3. Ahn K, et al. A novel mechanistic class of fatty acid amide hydrolase inhibitors with remarkable selectivity. Biochemistry. 2007; 46:13019–13030. [PubMed: 17949010]
4. Jo E, et al. S1P1-selective in vivo-active agonists from high-throughput screening: off-the-shelf chemical probes of receptor interactions, signaling, and fate. Chem Biol. 2005; 12:703–715. [PubMed: 15975516]
5. Dolma S, Lessnick SL, Hahn WC, Stockwell BR. Identification of genotype-selective antitumor agents using synthetic lethal chemical screening in engineered human tumor cells. Cancer Cell. 2003; 3:285–296. [PubMed: 12676586]
6. Galperin MY, Koonin EV. 'Conserved hypothetical' proteins: prioritization of targets for experimental study. Nucleic Acids Res. 2004; 32:5452–5463. [PubMed: 15479782]
7. Woitach JT, Zhang M, Niu CH, Thorgeirsson SS. A retinoblastoma-binding protein that affects cell-cycle control and confers transforming ability. Nat Genet. 1998; 19:371–374. [PubMed: 9697699]
8. Rao M, Sockanathan S. Transmembrane protein GDE2 induces motor neuron differentiation in vivo. Science. 2005; 309:2212–2215. [PubMed: 16195461]
9. Semba S, et al. Biological functions of mammalian NIT1, the counterpart of the invertebrate NITFHIT rosetta stone protein, a possible tumor suppressor. J Biol Chem. 2006
10. Evans MJ, Cravatt BF. Mechanism-based profiling of enzyme families. Chem Rev. 2006; 106:3279–3301. [PubMed: 16895328]
11. Cravatt BF, Wright AT, Kozarich JW. Activity-Based Protein Profiling: From Enzyme Chemistry to Proteomic Chemistry. Annu Rev Biochem. 2008; 77:383–414. [PubMed: 18366325]
12. Jessani N, Liu Y, Humphrey M, Cravatt BF. Enzyme activity profiles of the secreted and membrane proteome that depict cancer invasiveness. Proc. Natl. Acad. Sci. U.S.A. 2002; 99:10335–10340. [PubMed: 12149457]
13. Jessani N, et al. A streamlined platform for high-content functional proteomics of primary human specimens. Nat Methods. 2005; 2:691–697. [PubMed: 16118640]
14. Joyce JA, et al. Cathepsin cysteine proteases are effectors of invasive growth and angiogenesis during multistage tumorigenesis. Cancer Cell. 2004; 5:443–453. [PubMed: 15144952]
15. Adam GC, Sorensen EJ, Cravatt BF. Proteomic profiling of mechanistically distinct enzyme classes using a common chemotype. Nat Biotechnol. 2002; 20:805–809. [PubMed: 12091914]
16. Greenbaum DC, et al. A role for the protease falcipain 1 in host cell invasion by the human malaria parasite. Science. 2002; 298:2002–2006. [PubMed: 12471262]

17. Blankman JL, Simon GS, Cravatt BF. A Comprehensive Profile of Brain Enzymes that Hydrolyze the Endocannabinoid 2-Arachidonoylglycerol. Chem. Biol. 2007; 14:1347–1356. [PubMed: 18096503]
18. Barglow KT, Cravatt BF. Substrate mimicry in an activity-based probe that targets the nitrilase family of enzymes. Angew Chem Int Ed Engl. 2006; 45:7408–7411. [PubMed: 17036295]
19. Leung D, Hardouin C, Boger DL, Cravatt BF. Discovering potent and selective reversible inhibitors of enzymes in complex proteomes. Nat. Biotechnol. 2003; 21:687–691. [PubMed: 12740587]
20. Chiang KP, Niessen S, Saghatelian A, Cravatt BF. An enzyme that regulates ether lipid signaling pathways in cancer annotated by multidimensional profiling. Chem Biol. 2006; 13:1041–1050. [PubMed: 17052608]
21. Li W, Blankman JL, Cravatt BF. A functional proteomic strategy to discover inhibitors for uncharacterized hydrolases. J. Am. Chem. Soc. 2007; 129:9594–9595. [PubMed: 17629278]
22. Vorobiev SM, et al. Crystal structure of human retinoblastoma binding protein 9. Proteins. 2008; 74:526–529. [PubMed: 19004028]
23. Patricelli MP, Giang DK, Stamp LM, Burbaum JJ. Direct visualization of serine hydrolase activities in complex proteome using fluorescent active site-directed probes. Proteomics. 2001; 1:1067–1071. [PubMed: 11990500]
24. Liu Y, Patricelli MP, Cravatt BF. Activity-based protein profiling: the serine hydrolases. Proc. Natl. Acad. Sci. U.S.A. 1999; 96:14694–14699. [PubMed: 10611275]
25. Hoover HS, Blankman JL, Niessen S, Cravatt BF. Selectivity of inhibitors of endocannabinoid biosynthesis evaluated by activity-based protein profiling. Bioorg Med Chem Lett. 2008; 18:5838–5841. [PubMed: 18657971]
26. Saario SM, et al. Characterization of the sulfhydryl-sensitive site in the enzyme responsible for hydrolysis of 2-arachidonoyl-glycerol in rat cerebellar membranes. Chem Biol. 2005; 12:649–656. [PubMed: 15975510]
27. Feng BY, Shelat A, Doman TN, Guy RK, Shoichet BK. High-throughput assays for promiscuous inhibitors. Nat Chem Biol. 2005; 1:146–148. [PubMed: 16408018]
28. Feng BY, et al. A high-throughput screen for aggregation-based inhibition in a large compound library. J Med Chem. 2007; 50:2385–2390. [PubMed: 17447748]
29. Feng BY, Shoichet BK. A detergent-based assay for the detection of promiscuous inhibitors. Nat Protoc. 2006; 1:550–553. [PubMed: 17191086]
30. Boon-Unge K, et al. Emetine regulates the alternative splicing of Bcl-x through a protein phosphatase 1-dependent mechanism. Chem Biol. 2007; 14:1386–1392. [PubMed: 18096507]
31. Keiser MJ, et al. Relating protein pharmacology by ligand chemistry. Nat Biotechnol. 2007; 25:197–206. [PubMed: 17287757]
32. Grollman AP. Structural Basis for Inhibition of Protein Synthesis by Emetine and Cycloheximide Based on an Analogy between Ipecac Alkaloids and Glutarimide Antibiotics. Proc Natl Acad Sci U S A. 1966; 56:1867–1874. [PubMed: 16591432]
33. Gupta RS, Siminovitch L. The molecular basis of emetine resistance in Chinese hamster ovary cells: alteration in the 40S ribosomal subunit. Cell. 1977; 10:61–66. [PubMed: 837444]
34. Monks TJ, Jones DC. The metabolism and toxicity of quinones, quinonimines, quinone methides, and quinone-thioethers. Curr Drug Metab. 2002; 3:425–438. [PubMed: 12093358]
35. Hayes JD, Flanagan JU, Jowsey IR. Glutathione transferases. Annu Rev Pharmacol Toxicol. 2005; 45:51–88. [PubMed: 15822171]
36. Yan XD, Pan LY, Yuan Y, Lang JH, Mao N. Identification of platinum-resistance associated proteins through proteomic analysis of human ovarian cancer cells and their platinum-resistant sublines. J Proteome Res. 2007; 6:772–780. [PubMed: 17269733]
37. Board PG, et al. Identification, characterization, and crystal structure of the omega class glutathione transferases. J. Biol. Chem. 2000; 275:24798–24806. [PubMed: 10783391]
38. Whitbread AK, et al. Characterization of the omega class of glutathione transferases. Methods Enzymol. 2005; 401:78–99. [PubMed: 16399380]

39. Zhang K, Wong KP. Glutathione conjugation of chlorambucil: measurement and modulation by plant polyphenols. Biochem J. 1997; 325(Pt 2):417–422. [PubMed: 9230122]
40. Adam GC, Sorensen EJ, Cravatt BF. Trifunctional chemical probes for the consolidated detection and identification of enzyme activities from complex proteomes. Mol. Cell. Proteomics. 2002; 1:828–835. [PubMed: 12438565]
41. Liu S, Cerione RA, Clardy J. Structural basis for the guanine nucleotide-binding activity of tissue transglutaminase and its regulation of transamidation activity. Proc Natl Acad Sci U S A. 2002; 99:2743–2747. [PubMed: 11867708]
42. Board PG, et al. S-(4-Nitrophenacyl)glutathione is a specific substrate for glutathione transferase omega 1−1. Anal Biochem. 2008; 374:25–30. [PubMed: 18028863]
43. Torta F, Usuelli V, Malgaroli A, Bachi A. Proteomic analysis of protein S-nitrosylation. Proteomics. 2008; 8:4484–4494. [PubMed: 18846506]
44. Poole LB, Nelson KJ. Discovering mechanisms of signaling-mediated cysteine oxidation. Curr Opin Chem Biol. 2008; 12:18–24. [PubMed: 18282483]
45. Vila A, et al. Identification of protein targets of 4-hydroxynonenal using click chemistry for ex vivo biotinylation of azido and alkynyl derivatives. Chem Res Toxicol. 2008; 21:432–444. [PubMed: 18232660]
46. Hafner M, et al. Inhibition of cytohesins by SecinH3 leads to hepatic insulin resistance. Nature. 2006; 444:941–944. [PubMed: 17167487]
47. Antczak C, Radu C, Djaballah H. A profiling platform for the identification of selective metalloprotease inhibitors. J Biomol Screen. 2008; 13:285–294. [PubMed: 18349423]
48. Patricelli MP, et al. Functional interrogation of the kinome using nucleotide acyl phosphates. Biochemistry. 2007; 46:350–358. [PubMed: 17209545]
49. Chandonia JM, Brenner SE. The impact of structural genomics: expectations and outcomes. Science. 2006; 311:347–351. [PubMed: 16424331]

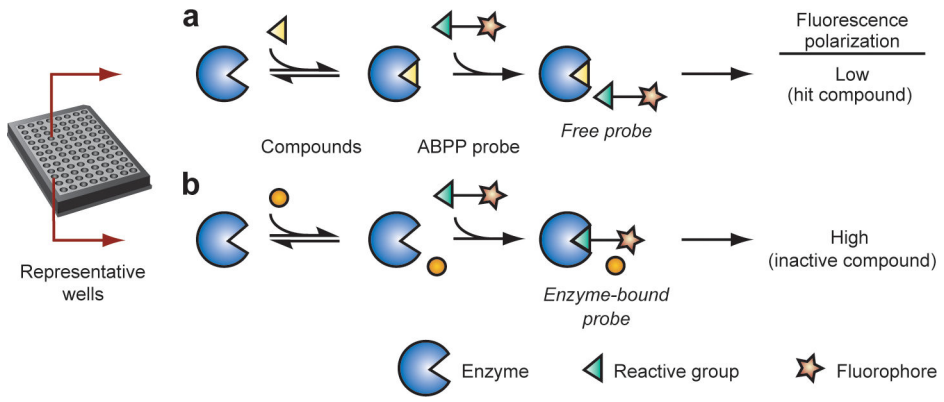


**Figure 1.**

Schematic representation of the FluoPol-ABPP platform. An enzyme is dispensed into a 384-well plate, and a different test compound is added to each well. Shown are representative wells where the test compound is an inhibitor of the enzyme (**a**) or is inactive (**b**). A fluorescent ABPP probe is then dispensed to all wells, and the plate incubated for a fixed time interval. The reaction of the probe with uninhibited enzyme (**b**), but not inhibited enzyme (**a**), will greatly increase the apparent mass of the probe, resulting in the maintenance of a strong FluoPol signal.

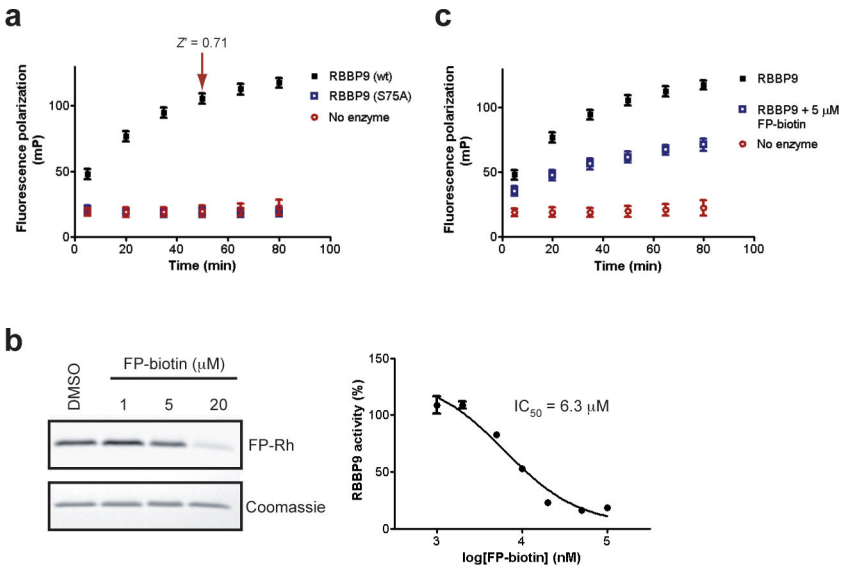


**Figure 2.**

Optimization and validation of the FluoPol-ABPP platform for RBBP9. (**a**) RBBP9 (2 μM) and FP-rhodamine (75 nM) generated a strong, time-dependent increase in FluoPol signal. No labeling was observed in the absence of enzyme or with the catalytically-dead S75A mutant RBBP9. The indicated 45-minute time point ($Z'$ = 0.71) prior to reaction completion was selected for HTS. Error bars represent s.d.. (**b**) Under these conditions, FP-biotin (30 min pre-incubation) inhibited FP-rhodamine labeling of RBBP9 with an $IC_{50}$ value of 6.3 μM as determined by gel-based competitive ABPP. Left panel, fluorescent gel is shown in gray scale. Right panel, error bars represent s.e.m. (**c**) FP-biotin (5 μM) gave an ∼50% reduction in the RBBP9-generated FluoPol signal. Error bars represent s.d.

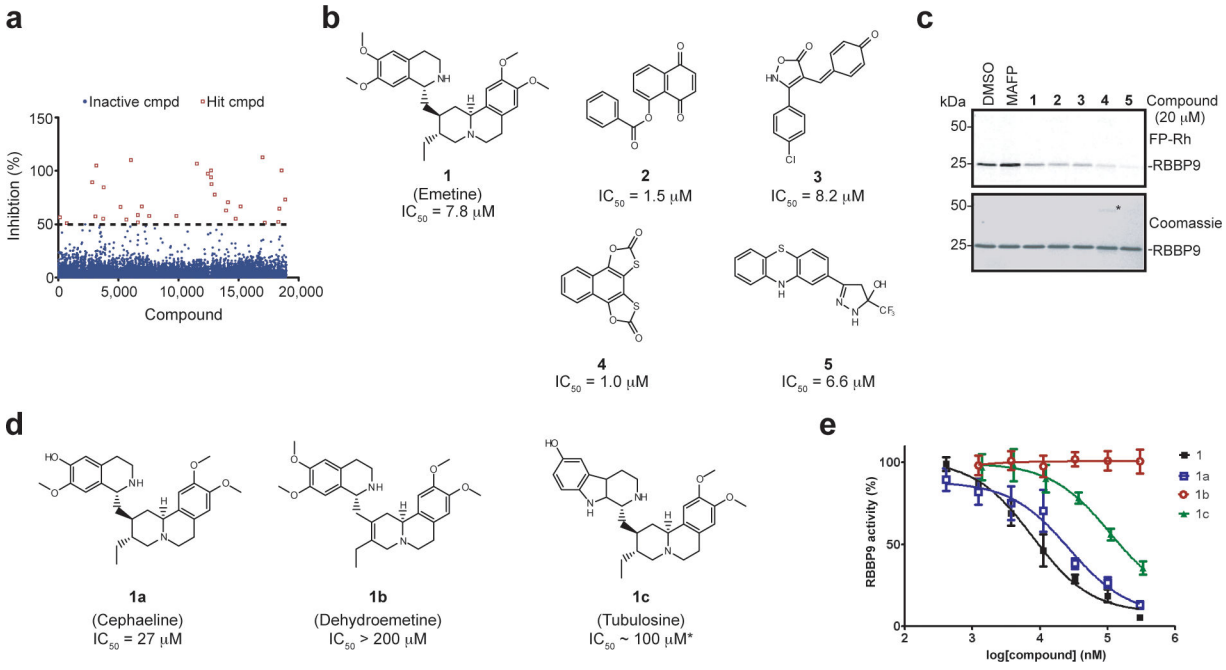


**Figure 3.**

Identification of RBBP9 primary hits. (**a**) A screen of 18,974 compounds identified 35 hits that reduced the FluoPol signal of FP-rhodamine labeling of RBBP9 by > 50% relative to control reactions run in the absence of added compound. (**b**) Structures of representative primary hits. (**c**) Inhibition of FP-rhodamine labeling of RBBP9 by representative compound hits (20 μM, 30 min preincubation) as determined by gel-based competitive ABPP (upper panel). Compound **4** covalently dimerized RBBP9 as determined by protein staining (Coomaissee blue) (lower panel, asterisk). (**d** and **e**) Structures of emetine analogues (**d**) and $IC_{50}$ curves for RBBP9 (**e**) as determined by gel-based competitive ABPP. Asterisk in **d** notes compound insolubility at high concentrations (> 300 μM) precluded accurate $IC_{50}$ determination. Error bars in **e** represent s.e.m.

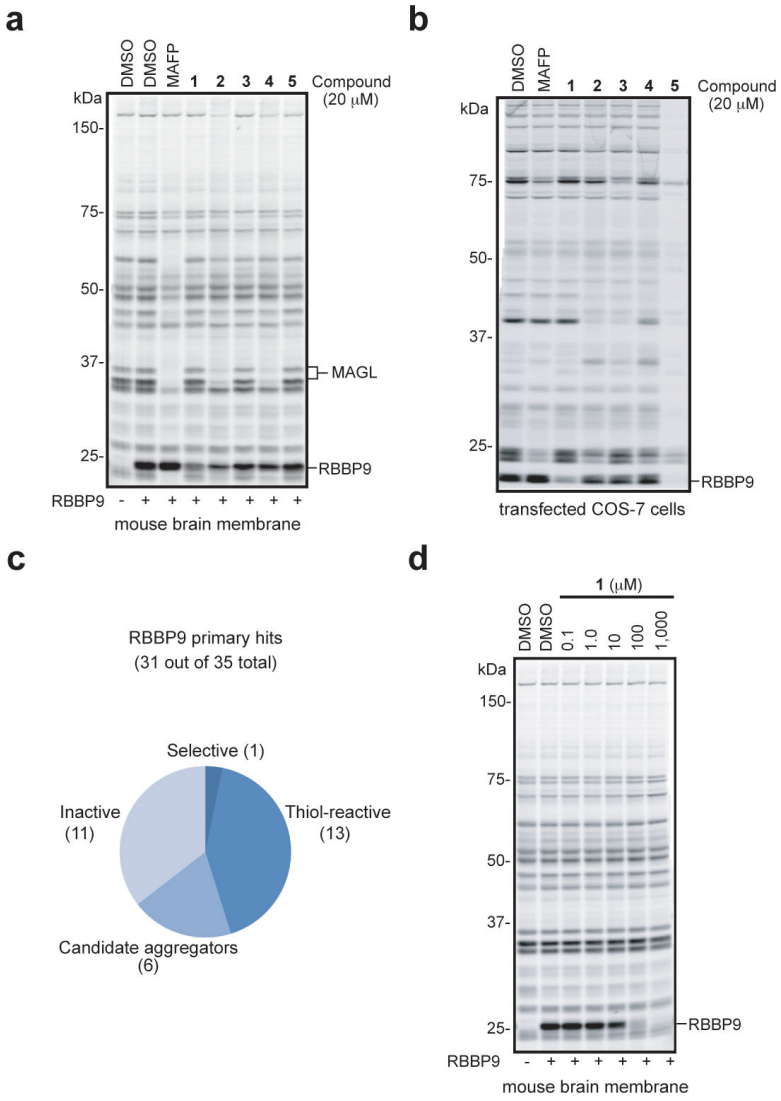


**Figure 4.**

Competitive ABPP in proteomes identifies emetine (**1**) as a selective inhibitor of RBBP9. (**a**) Evaluation of representative hits (20 μM, 30 min preincubation) by competitive ABPP in the mouse brain membrane proteome (1 mg/mL proteome; 1 μM FP-rhodamine, 10 min, room temperature). Recombinant human RBBP9 (400 nM) was doped into this proteome for comparison. (**b**) Competitive ABPP of representative hits in RBBP9-transfected COS-7 cytosolic proteomes (1 mg/mL protein). RBBP9-transfected cells expressed high levels of active RBBP9 compared to mock-transfected cells, as judged by ABPP (Supplementary Fig. 3). (**c**) Primary hits can be segregated into four general categories based on performance in competitive proteomic ABPP assays. (**d**) Concentration-dependent effects of emetine (**1**) on FP-rhodamine labeling of mouse brain serine hydrolases. Note that emetine selectively inhibits RBBP9 labeling at concentrations up to 1 mM.

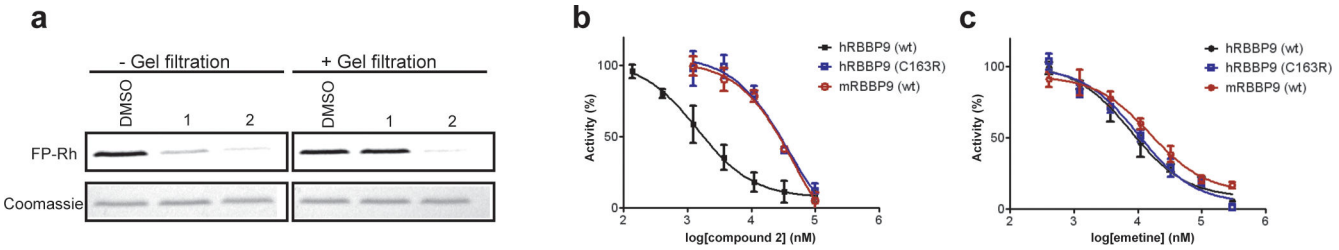


**Figure 5.**

Mechanistic characterization of RBBP9 inhibitors. (**a**) RBBP9 (2 μM) was incubated (30 min) with DMSO, emetine (500 μM), or compound **2** (50 μM). Each reaction was then split into two fractions - one fraction was reacted directly with FP-rhodamine (left panels), and the other fraction was passaged over a Sephadex G-25M column and then reacted with FP-rhodamine (right panels) to assess the reversibility of inhibition. (**b** and **c**) $IC_{50}$curves for compound **2** (**b**) and emetine (**c**) with human RBBP9 (wt), the C163R mutant of human RBBP9, and mouse RBBP9 as determined by gel-based competitive ABPP. Error bars represent s.e.m.

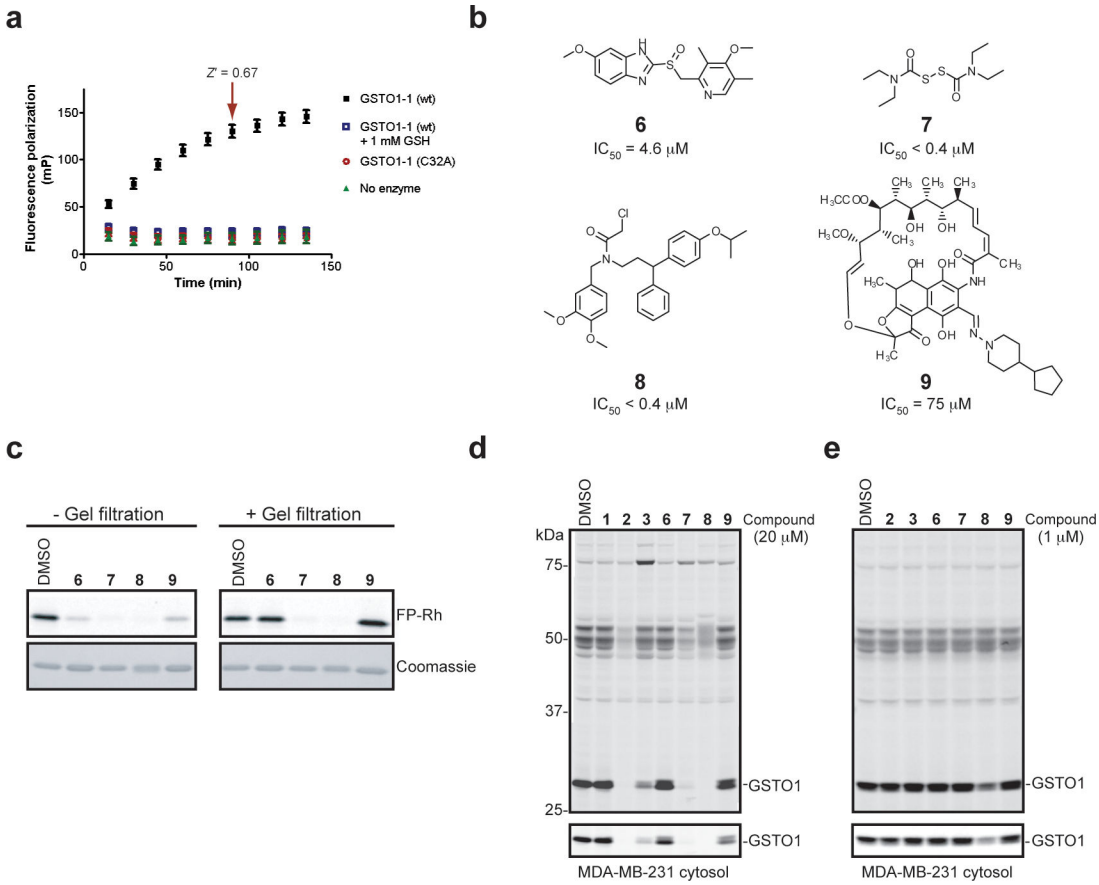


**Figure 6.**

FluoPol-ABPP platform identifies a selective inhibitor of GSTO1. (**a**) GSTO1 (1 μM) and SE-rhodamine (75 nM) generated a strong, time-dependent increase in FluoPol signal. No labeling was observed in the absence of enzyme, with a catalytically-dead C32A mutant GSTO1 (1 μM), or in the presence of glutathione (1 mM), which has been shown to react with C3237. The indicated 90-minute time point (*Z*' = 0.67) prior to reaction completion was selected for HTS. Error bars represent s.d. (**b**) Structures of representative primary hits and $IC_{50}$ values for inhibition of GSTO1 as determined by competitive gel-based ABPP (400 nM GSTO1, 1 μM SE-rhodamine, 20 min, room temperature). (**c**) Assessing the reversibility of GSTO1 inhibition. GSTO1 (2 μM) was incubated with DMSO or the indicated compound for 30 min **6** (280 μM)**, 7** (28 μM), **8** (28 μM) or **9** (280 μM). Each reaction was then split into two fractions - one fraction was reacted directly with SE-rhodamine (left panels), and the other fraction was passaged over a Sephadex G-25M column and then reacted with SE-rhodamine (right panels). (**d** and **e**) Evaluation of compounds at 20 μM (**d**) or 1 μM (**e**) by competitive ABPP in the soluble proteome of MDA-MB-231 breast cancer cells (2 mg/mL protein, 5 μM FP-rhodamine, 1 hr, room temperature). Lower panels in **d** and **e** represent reduced-intensity images of the 30 kDa region of the upper panels where endogenous GSTO1 migrates.